Inorganic Chemistry
Article

Inorg. Chem. **2009**, *48*, 6371–6379 **6371**
DOI: 10.1021/ic802115n

Catalytic Properties of Cobalt(III)−Oxo Cubanes in the TBHP Oxidation of Benzylic Alcohols

Rajesh Chakrabarty,[†] Purabi Sarmah, Bapan Saha, Stutee Chakravorty, and Birinchi K. Das*

Department of Chemistry, Gauhati University, Guwahati 781 014, India. [†]Present address: Department of Inorganic and Physical Chemistry, Indian Institute of Science, Bangalore 560 012, India.

Received November 4, 2008

Two series of oxo-bridged Co(III) complexes of the type $Co_4O_4(O_2CC_6H_4\text{-}X)_4(py)_4$ (**1**) and $Co_4O_4(O_2CC_6H_4\text{-}X)_4(4\text{-}Mepy)_4$ (**2**), where X = H (**a**), Me (**b**), MeO (**c**), Cl (**d**), NO_2 (**e**), have been synthesized and characterized in detail. The molecular structures of the complexes consist of a cubelike $Co_4(\mu_3\text{-}O)_4$ core having Co and O atoms at alternate vertices with carboxylato ligands bridging the Co^{3+} ions along four face diagonals of the approximate cube. Nitrogen atoms from pyridyl ligands complete the distorted-octahedral coordination around each Co(III). These neutral Co(III) complexes undergo a nearly reversible one-electron oxidation involving the redox couple $[Co_4^{III}(\mu_3\text{-}O)_4]^{4+} \leftrightarrow [Co_3^{III}Co^{IV}(\mu_3\text{-}O)_4]^{5+}$ at potentials (∼0.7−1.0 V) that linearly depend on the electronic influence of X. The cobalt(III) clusters of types **1** and **2** have been found to effectively promote the TBHP oxidation of benzylic alcohols under homogeneous conditions to produce the corresponding carbonyl compounds.

Introduction

The chemistry of oxo-bridged transition-metal clusters continues to attract a great deal of interest and has immensely grown during the last two decades. These metal clusters have been found to exhibit complex and varied structural motifs,[1] unusual magnetic behavior,[1] and interesting catalytic properties.[2] Some of these compounds have been projected as new molecular materials or model systems for the polymetallic active sites in metallobiomolecules.[3] Utilizing the ability of the ligand system RCO_2^-/L (L = N-, O-donor ligands) to assemble oligonuclear metal clusters, it has been possible to form various tetrameric cobalt clusters possessing the cubane (**I**) as well as defect dicubane (**II**) geometries.[4−18]

*To whom correspondence should be addressed. E-mail: das_bk@rediffmail.com. Tel: +91 (0)361 2570535. Fax: +91 (0)361 2700311.

(1) (a) Winpenny, R. E. P. In *Comprehensive Coordination Chemistry*; McCleverty, J. A., Meyer, T. J., Eds.; Pergamon Press: Oxford, U.K., 2004; Vol. 7, Chapter 7.3, pp 125−175. (b) Winpenny, R. E. P. Adv. Inorg. Chem. 2001, *52*, 1–111. (c) Gatteschi, D.; Sessoli, R.; Cornia, A. In Comprehensive Coordination Chemistry; McCleverty, J. A., Meyer, T. J., Eds.; Pergamon Press: Oxford, U.K., 2004; Vol. 7, Chapter 7.13, pp 779−813.

(2) (a) Sumner, C. E., Jr.; Morrill, K. A.; Howell, J. S.; Little, J. *Inorg. Chem.* **2008**, *47*, 2190–2195. (b) Lassahn, P.-G.; Lozan, V.; Timco, G. A.; Christian, P.; Janiak, C.; Winpenny, R. E. P. *J. Catal.* **2004**, *222*, 260–267. (c) Carrell, T. G.; Cohen, S.; Dismukes, G. C. *J. Mol. Catal. A: Chem.* **2002**, *187*, 3–15. (d) Chavan, S. A.; Srinivas, D.; Ratnasamy, P. *J. Catal.* **2001**, *204*, 409–419.

(3) For reviews see: (a) Cady, C. W.; Crabtree, R. H.; Brudvig, G. W. *Coord. Chem. Rev.* **2008**, *252*, 444–455. (b) Solomon, E. I.; Sarangi, R.; Woertink, J. S.; Augustine, A. J.; Yoon, J.; Ghosh, S. *Acc. Chem. Res.* **2007**, *40*, 581–591. (c) Mukhopadhyay, S.; Mandal, S. K.; Bhaduri, S.; Armstrong, W. H. *Chem. Rev.* **2004**, *104*, 3981–4026. (d) Lippard, S. J.; Tshuva, E. Y. *Chem. Rev.* **2004**, *104*, 987–1012. (e) Que, L., Jr. *J. Chem. Soc., Dalton Trans.* **1997**, 3933–3940. (f) Holm, R. H; Kennepohl, P.; Solomon, E. I. *Chem. Rev.* **1996**, *96*, 2239–2314. (g) Wallar, B. J; Lipscomb, J. D. *Chem. Rev.* **1996**, *96*, 2625–2657.

(4) (a) Papaefstathiou, G. S.; Escuer, A.; Font-Bardía, M.; Perlepes, S. P.; Solans, X.; Vicente, R. *Polyhedron* **2002**, *21*, 2027–2032. (b) Serna, Z. E.; Urtiaga, M. K.; Barandika, M. G.; Cortés, R.; Martin, S.; Lezama, L.; Arriortua, M. I.; Rojo, T. *Inorg. Chem.* **2001**, *40*, 4550–4555.

(5) (a) Lin, Z.; Li, Z.; Zhang, H. *Cryst. Growth Des.* **2007**, *7*, 589–591. (b) Berry, J. F.; Cotton, F. A.; Liu, C. Y.; Lu, T.; Murillo, C. A.; Tsukerblat, B. S.; Villagrán, D.; Wang, X. *J. Am. Chem. Soc.* **2005**, *127*, 4895–4902. (c) Dimitrou, K.; Sun, J.-S.; Folting, K.; Christou, G. *Inorg. Chem.* **1995**, *34*, 4160–4166.

(6) (a) Galloway, K. W.; Whyte, A. M.; Wernsdorfer, W.; Sanchez-Benitez, J.; Kamenev, K. V.; Parkin, A.; Peacock, R. D.; Murrie, M. *Inorg. Chem.* **2008**, *47*, 7438–7442. (b) Zeng, M.-H.; Yao, M.-X.; Liang, H.; Zhang, W.-X.; Chen, X.-M. *Angew. Chem., Int. Ed.* **2007**, *46*, 1832–1835. (c) Murrie, M.; Teat, S. J.; Stœckli-Evans, H.; Güdel, H. U. *Angew. Chem., Int. Ed.* **2003**, *42*, 4653–4656.

(7) Dimitrou, K.; Folting, K.; Streib, W. E.; Christou, G. *J. Am. Chem. Soc.* **1993**, *115*, 6432–6433.

(8) Beattie, J. K.; Hambley, T. W.; Klepetko, J. A.; Masters, A. F.; Turner, P. *Polyhedron* **1998**, *17*, 1343–1354.

(9) Ama, T.; Rashid, M. M.; Yonemura, T.; Kawaguchi, H.; Takeuchi, A.; Yasui, T. *Coord. Chem. Rev.* **2000**, *198*, 101–116.

(10) Ama, T.; Okamoto, K.; Yonemura, T.; Kawaguchi, H.; Takeuchi, A.; Yasui, T. *Chem. Lett.* **1997**, 1189–1190.

(11) Bertrand, J. A.; Hightower, T. C. *Inorg. Chem.* **1973**, *12*, 206–210.

(12) Wang, R.; Hong, M; Su, W.; Cao, R. *Acta Crystallogr.* **2001**, *E57*, m325–m665.

(13) Berchin, E. K.; Harris, S. G.; Parsons, S.; Winpenny, R. E. P. *J. Chem. Soc., Chem. Commun.* **1996**, 1439–1440.

(14) Gubina, K. E.; Ovchynnikov, V. A.; Swiatek-Kozlowska, J.; Amirkhanov, V. M.; Sliva, T. Y.; Domasevitch, K. V. *Polyhedron* **2002**, *21*, 963–967.

(15) Aromí, G.; Batsanov, A. S.; Christian, P.; Helliwell, M.; Parkin, A.; Parsons, S.; Timco, G. A.; Winpenny, R. E. P. *Chem. Eur. J.* **2003**, *9*, 5142–5161.

(16) He, C.; Lippard, S. *J. Am. Chem. Soc.* **2000**, *122*, 184–185.

(17) Zhao, H.; Bacsa, J.; Dunbar, K. R. *Acta Crystallogr.* **2004**, *E60*, m637–m640.

(18) Chakrabarty, R.; Bora, S. J.; Das, B. K. *Inorg. Chem.* **2007**, *46*, 9450–9462.

Published on Web 06/23/2009

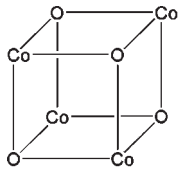

Cubane (I)

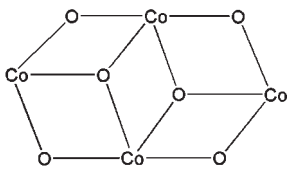

Defect dicubane (II)

We have been studying cobalt(III) cubanelike complexes of the type $Co_4O_4(O_2CR)_4L_4$, where R is methyl or an aryl group and L is either pyridine or a substituted pyridine ligand, as these structurally robust clusters have shown promising catalytic properties in the oxidation of various organic substrates such as alkyl aromatics, alcohols, and terpenoids under environmentally friendly conditions.[18−20] In this context, we have become interested in examining how the nature of R and L in the tetrameric complexes can influence their physicochemical properties, which in turn may lead to changes in their catalytic behavior. A heterogeneous catalyst prepared by immobilizing the complex $Co_4O_4(O_2CCH_3)_4(py)_4$ was earlier found to show promising catalytic activity in the TBHP oxidation of alcohols.[19] With a view to examining the homogeneous catalytic activity of the cobalt(III)−oxo cubanes in alcohol oxidation, we have presently prepared several new complexes having substituted benzoates as ligands. Herein we describe the synthesis and properties of clusters of types $Co_4(\mu_3\text{-}O)_4(\mu\text{-}O_2CC_6H_4\text{-}X)_4(py)_4$ (**1**) and $Co_4(\mu_3\text{-}O)_4(\mu\text{-}O_2CC_6H_4\text{-}X)_4(4\text{-}Mepy)_4$ (**2**), where X=H (**a**), Me (**b**), MeO (**c**), Cl (**d**), NO_2 (**e**). We also demonstrate that these compounds act as effective homogeneous catalysts in the TBHP oxidation of a few benzylic alcohols to selectively produce the corresponding carbonyl compounds in yields which are influenced by the nature of the ligands present in the complexes.

Experimental Section

Materials. All materials, including $Co(NO_3)_2\cdot 6H_2O$, hydrogen peroxide (30%, v/v), and 4-methylpyridine (E. Merck, India), pyridine (Qualigens, India), tetrabutylammonium perchlorate (TBAP; E. Merck, Germany), benzyl alcohol (E. Merck, India), benzhydrol (Loba Chemie, India), 1-phenylethanol, 1-phenyl-1-propanol, and 4-chloro- and 4-nitrobenzyl alcohols (Aldrich, USA) were used as received without further purification. Sodium salts of the aromatic carboxylic acids (NaO_2CAr) were prepared by neutralizing the acids with sodium hydroxide; evaporation of the neutralized solutions, recrystallization of the crude products, and drying at elevated temperature gave pure products. Methanol and acetonitrile used for synthesis and catalytic studies, respectively, were of reagent grade. Dichloromethane used for spectral and electrochemical studies was distilled after drying over P_4O_{10}.

Measurements. Fourier transform infrared (FT-IR) and solution electronic spectra were recorded on PerkinElmer RX1 and Lambda 40 spectrophotometers, respectively. C, H, N analyses were done using a PerkinElmer 2400 Series II CHNS/O Analyzer. ^{1}H NMR and electrospray ionization mass (ESI-MS) measurements were made using Bruker Advanced 400 MHz and Bruker Daltonics (Esquire 300 Plus ESI model) instruments, respectively. All electrochemical measurements were carried out in dichloromethane using scan rates in the range of 5−20 mVs^{-1} on a EG&G PAR Model 253 VersaStat potentiostat/galvanostat having a three-electrode setup consisting of a glassy-carbon working electrode, a platinum-wire auxiliary electrode, and a saturated calomel electrode (SCE) reference combined with Electrochemical Analysis 270 software for recording the voltammograms. For DPV experiments 50 ms pulses were used. Oxygen was rigorously removed from the solutions of the samples by purging with dry N_2 gas of high purity. Ferrocene was used as an internal standard for determining the stoichiometry of the electron-transfer processes. Gas chromatography was done by using a Varian 450-GC instrument equipped with an FID detector and a CP-Sil 8 CB capillary column. Retention times of reaction products were confirmed by comparison with authentic samples.

Preparation of Complexes. $Co_4(\mu_3\text{-}O)_4(\mu\text{-}O_2CC_6H_5)_4(py)_4$ (1a). $Co(NO_3)_2\cdot 6H_2O$ (2.90 g, 10 mmol) and sodium benzoate (2.88 g, 20 mmol) were stirred in methanol (20 mL) at reflux temperature, and pyridine (0.8 mL, 10 mmol) was added to the mixture. To the reaction mixture was slowly added 30% hydrogen peroxide (v/v, 5 mL, ∼50 mmol) dropwise, and stirring under reflux conditions was continued for 4 h. The olive green product that precipitated out during the reaction was washed thoroughly with water and then with small portions of methanol. It was then dried in a vacuum desiccator over fused $CaCl_2$. Yield: 2.16 g (79% based on cobalt). Anal. Calcd (found) for $C_{48}H_{40}N_4O_{12}Co_4$: C, 52.38 (51.46); H, 3.66 (3.08); N, 5.09 (5.34). ESI-MS (m/z, (%)): 1101.07 (100) $[M]^+$. IR data (KBr pellet, ν_{max}/cm^{-1}): 3426 (m, br), 1635 (w), 1605 (w), 1525 (vs), 1485 (m), 1450 (m), 1382 (vs), 1212 (w), 1173 (w), 1070 (m), 1024 (w), 847 (w), 761 (w), 721 (s), 691 (s), 637 (m), 585 (s) 486 (m).

$Co_4(\mu_3\text{-}O)_4(\mu\text{-}O_2CC_6H_4\text{-}4\text{-}Me)_4(py)_4$ (1b). The method was the same as for **1a**, but sodium benzoate was replaced by sodium 4-methylbenzoate (3.16 g, 20 mmol). Yield: 2.20 g (76% based on cobalt). Anal. Calcd (found) for $C_{52}H_{48}N_4O_{12}Co_4$: C, 54.00 (53.76); H, 4.18 (4.29); N, 4.84 (5.02). ESI-MS (m/z, (%)): 1157.07 (100) $[M]^+$. IR data (KBr pellet, ν_{max}/cm^{-1}): 3400 (m), 3031 (w), 2921 (w), 1637 (w), 1607 (s), 1583 (m), 1519(vs), 1484 (s), 1449 (s), 1384(vs), 1292 (w), 1246 (w), 1212 (s), 1176 (s), 1153 (w), 1070 (m), 1046 (w), 1019 (m), 850 (m), 786 (m), 765 (s), 690 (s), 640 (s), 582 (s), 479 (m), 457 (m).

$Co_4(\mu_3\text{-}O)_4(\mu\text{-}O_2CC_6H_4\text{-}4\text{-}OMe)_4(py)_4$ (1c). The method was the same as for **1a**, but sodium benzoate was replaced by sodium 4-methoxybenzoate (3.48 g, 20 mmol). Yield: 2.6 g (85% based on cobalt). Anal. Calcd (found) for $C_{52}H_{48}N_4O_{16}Co_4$: C, 51.16 (51.01); H, 3.96 (3.41); N, 4.59 (4.82). ESI-MS (m/z, (%)): 1221.13 (100) $[M]^+$. IR data (KBr pellet, ν_{max}/cm^{-1}): 3409 (w), 3074 (w), 2956 (w), 2933 (w), 2836 (w), 1605 (s), 1587 (s), 1517 (s), 1484 (m), 1449 (s), 1382 (vs), 1309 (m), 1252 (s), 1212 (m), 1170 (s), 1104 (m), 1070 (m), 1026 (s), 851 (s), 780 (s), 760 (m), 692 (s), 647 (s), 633 (s), 587 (s), 511 (w), 456 (w), 429 (w).

$Co_4(\mu_3\text{-}O)_4(\mu\text{-}O_2CC_6H_4\text{-}4\text{-}Cl)_4(py)_4$ (1d). The method was the same as for **1a**, but sodium benzoate was replaced by sodium 4-chlorobenzoate (3.57 g, 20 mmol). Yield: 2.1 g (68% based on cobalt). Anal. Calcd (found) for $C_{48}H_{36}N_4O_{12}Cl_4Co_4$: C, 46.55 (46.11); H, 2.93 (2.35); N, 4.52 (4.91). ESI-MS (m/z, (%)): 1238.87 (100) $[M]^+$. IR data (KBr pellet, ν_{max}/cm^{-1}): 3368(m, br), 3074 (w), 2925 (w), 2820 (w), 1635 (w), 1605 (m), 1584 (vs), 1526 (vs), 1485 (s), 1449 (s), 1388 (vs), 1279 (w), 1244 (w), 1212 (m), 1169 (m), 1141 (m), 1087 (s), 1070 (m), 1047 (w), 1014 (s), 850 (s), 771 (s), 733 (w), 690 (s), 634 (m), 587 (m), 566 (m), 479 (m), 455 (w), 424 (w).

$Co_4(\mu_3\text{-}O)_4(\mu\text{-}O_2CC_6H_4\text{-}4\text{-}NO_2)_4(py)_4$ (1e). The method was the same as for **1a**, but sodium benzoate was replaced by sodium 4-nitrobenzoate (3.78 g, 20 mmol). Yield: 2.1 g (66% based on cobalt). Anal. Calcd (found) for $C_{48}H_{36}N_8O_{20}Co_4$: C,

(19) Sarmah, P.; Chakrabarty, R.; Phukan, P.; Das, B. K. *J. Mol. Catal. A: Chem.* **2007**, *268*, 36–44.

(20) (a) Chakrabarty, R.; Das, B. K.; Clark, J. H. *Green Chem.* **2007**, *9*, 845–848. (b) Chakrabarty, R.; Kalita, D.; Das, B. K. *Polyhedron* **2007**, *26*, 1239–1244. (c) Chakrabarty, R.; Das, B. K. *J. Mol. Catal. A: Chem.* **2004**, *223*, 39–44.

45.02 (44.82); H, 2.83, (2.29); N, 8.75 (8.41). ESI-MS (m/z, (%)): 1280.67 (100) $[M]^+$. IR data (KBr pellet, ν_{max}/cm^{-1}): 3402 (m, br), 3053 (w), 2941 (w), 2850 (w), 1609 (m), 1538 (vs), 1487 (s), 1450 (s), 1392 (vs), 1344 (vs), 1243 (w), 1215 (m), 1170 (w), 1145 (s), 1106 (s), 1072 (s), 1049 (w), 1015 (s), 875 (s), 836 (s), 791 (m), 762 (m), 728 (s), 692 (s), 638 (s), 587 (s), 552 (m), 450 (w), 429(w).

The synthesis of complexes belonging to series **2** was also accomplished by following analogous procedures.

$Co_4(\mu_3\text{-}O)_4(\mu\text{-}O_2CC_6H_5)_4(4\text{-Mepy})_4$ (2a). The reaction of $Co(NO_3)_2\cdot 6H_2O$ (2.90 g, 10 mmol) and sodium benzoate (2.88 g, 20 mmol) in methanol (30 mL) led to a pink precipitate. Addition of 4-methylpyridine (0.98 mL, 10 mmol) to the reaction mixture caused a color change from pink to red. To the resultant red solution was slowly added 30% hydrogen peroxide (v/v, 5 mL, ~50 mmol) dropwise, whereupon the initial precipitate dissolved. Stirring was continued for 4 h to obtain an olive green precipitate. The precipitate was washed thoroughly with water and then with small portions of methanol. It was then dried in a vacuum desiccator over fused $CaCl_2$. Yield: 1.84 g (64% based on cobalt). Anal. Calcd (found) for $C_{52}H_{48}N_4O_{12}Co_4$: C, 54.00 (53.83); H, 4.18 (4.01); N, 4.84 (4.57). ESI-MS (m/z, (%)): 1157.07 $[M]^+$. IR data (KBr pellet, ν_{max}/cm^{-1}): 3397 (w), 3060 (w), 2973 (w), 2919 (w), 2856 (w), 1621 (s), 1589 (m), 1528 (vs), 1501 (s), 1447 (m), 1383 (vs), 1208 (m), 1173 (w), 1143 (w), 1068 (m), 1026 (m), 847 (w), 810 (s), 724 (s), 693 (m), 637 (s), 588 (s), 576 (s), 495 (m), 483 (w), 449 (w).

$Co_4(\mu_3\text{-}O)_4(\mu\text{-}O_2CC_6H_4\text{-}4\text{-}Me)_4(4\text{-Mepy})_4$ (2b). The method was the same as for **2a**, but with sodium benzoate replaced by sodium 4-methylbenzoate (3.16 g, 20 mmol). A small amount of olive green product precipitated out during the reaction. Upon overnight storage in a refrigerator, further precipitation occurred. Yield: 1.75 g (58% based on cobalt). Anal. Calcd (found) for $C_{56}H_{56}N_4O_{12}Co_4$: C, 55.46 (55.12); H, 4.65 (4.27); N, 4.62 (4.81). ESI-MS (m/z, (%)): 1213.20 (100) $[M]^+$. IR data (KBr pellet, ν_{max}/cm^{-1}): 3431 (w), 3064 (w), 3032 (w), 2921 (w), 2820 (w), 1620 (s), 1589 (m), 1527 (vs), 1396 (vs), 1229 (w), 1210 (w), 1177 (s), 1146 (m), 1107 (w), 1068 (w), 1039 (s), 846 (m), 811 (w), 764 (s), 694 (s), 640 (m), 590 (s), 494 (w), 477 (w), 453 (w).

$Co_4(\mu_3\text{-}O)_4(\mu\text{-}O_2CC_6H_4\text{-}4\text{-}OMe)_4(4\text{-Mepy})_4$ (2c). The method was the same as for **2a**, but with sodium benzoate replaced by sodium 4-methoxybenzoate (3.48 g, 20 mmol). A small amount (~0.33 g) of olive green product precipitated out during the reaction. More precipitation occurred upon cooling. Yield: 1.90 g (60% based on cobalt). Anal. Calcd (found) for $C_{56}H_{56}N_4O_{16}Co_4$: C, 52.68 (52.35); H, 4.42 (4.17); N, 4.39 (4.75). ESI-MS (m/z, (%)): 1277.27 (100) $[M]^+$. IR data (KBr pellet, ν_{max}/cm^{-1}): 3400 (w), 3073 (w), 3032 (w), 2930 (w), 2836 (w), 1604 (s), 1523 (s), 1457 (w), 1393 (vs), 1307 (w), 1252 (vs), 1172 (s), 1104 (w), 1029 (m), 850 (m), 812 (w), 777 (s), 698 (w), 646 (m), 634 (m), 495 (w).

$Co_4(\mu_3\text{-}O)_4(\mu\text{-}O_2CC_6H_4\text{-}4\text{-}Cl)_4(4\text{-Mepy})_4$ (2d). The method was the same as for **2a**, but with sodium benzoate replaced by sodium 4-chlorobenzoate (3.57 g, 20 mmol). Yield: 2.11 g (65% based on cobalt). Anal. Calcd (found) for $C_{52}H_{44}N_4O_{12}Cl_4Co_4$: C, 48.25 (48.01); H, 3.43 (3.14); N, 4.33 (4.69). ESI-MS (m/z, (%)): 1295.00 (100) $[M]^+$. IR data (KBr pellet, ν_{max}/cm^{-1}) for **2d**: 3401 (w), 3072 (w), 3052 (w), 2923 (w), 2820 (w), 1620 (m), 1592 (s), 1536 (vs), 1503 (m), 1488 (w), 1387 (vs), 1279 (w), 1228 (w), 1207 (m), 1169 (m), 1141 (w), 1087 (s), 1036 (m), 1015 (s), 849 (s), 811 (s), 770 (s), 719 (w), 688 (w), 647 (m), 632 (m), 589 (m), 566 (s), 494 (m), 478 (m).

$Co_4(\mu_3\text{-}O)_4(\mu\text{-}O_2CC_6H_4\text{-}4\text{-}NO_2)_4(4\text{-Mepy})_4$ (2e). The method was the same as for **2a**, but with sodium benzoate replaced by sodium 4-nitrobenzoate (3.78 g, 20 mmol). Yield: 1.70 g (51% based on cobalt). Anal. Calcd (found) for $C_{52}H_{44}N_8O_{20}Co_4$: C, 46.72 (46.27); H, 3.32 (3.19); N, 8.38 (8.81). ESI-MS (m/z, (%)): 1336.20 (100) $[M]^+$. IR data (KBr pellet, ν_{max}/cm^{-1}): 3399 (w), 3080 (w), 3052 (w), 2926 (w), 2853 (w), 1622 (s), 1538 (vs), 1392 (vs), 1344 (vs), 1210 (m), 1170 (w), 1143 (m), 1105 (m), 1069 (w), 1038 (w), 1014 (w), 873 (s), 836 (s), 815 (s), 791 (m), 725 (s), 639 (m), 586 (m), 522 (m), 496 (w).

Table 1. Crystallographic Data for **1a**·6MeOH·0.5H_2O and **2a**·3.5MeOH·5H_2O

	1a·6MeOH·0.5H_2O	**2a**·3.5MeOH·5H_2O
formula	$C_{48}H_{40}N_4O_{12}Co_4\cdot 6MeOH\cdot 0.5H_2O$	$C_{52}H_{48}N_4O_{12}Co_4\cdot 3.5MeOH\cdot 5H_2O$
mol wt	1300.81	1359.03
cryst syst; space group	triclinic; $P\bar{1}$	monoclinic; $C2/m$
T, K	293	293
a, Å	11.120(3)	23.730(8)
b, Å	14.859(3)	15.187(5)
c, Å	18.726(4)	20.724(7)
α, deg	87.64(4)	90
β, deg	86.17(4)	123.298(1)
γ, deg	73.17(4)	90
V, Å^3	2954.2(12)	6242.8(3)
Z; ρ_{calcd}, g cm^{-3}	2; 1.462	4; 1.316
μ(Mo Kα), mm^{-1}	1.177	1.108
no. of rflns collected/unique	26 474/10 030	48 960/5734
R_{int}	0.0351	0.1015
R1[a]	0.0419	0.0643
wR2	0.1012	0.1585
GOF on F^2	1.016	1.023
$\Delta\rho_{max,min}$, e Å^{-3}	0.632, −0.515	0.886, −0.344

[a] $R1 = \sum||F_o|-|F_c||/\sum|F_o|$. $wR2 = \{\sum[w(F_o^2-F_c^2)^2]/\sum[w(F_o^2)^2]\}^{1/2}$, where $w = 1/[\sigma^2(F_o^2)+(aP)^2+bP]$ and $P = [2F_c^2 + \mathrm{Max}(F_o^2,0)]/3$.

X-ray Crystallographic Studies. Suitable single crystals of **1a** were obtained by allowing a methanolic solution of the complex to evaporate slowly at room temperature. Since the crystals were found to lose crystallinity in air, the crystal was mounted in a capillary containing mother liquor. Single crystals of **2a** could be obtained by cooling the reaction mixture. X-ray diffraction data for crystalline samples of **1a** and **2a** were collected using Mo Kα radiation (0.710 73 Å) at 293 K on Bruker SMART APEX and Bruker KAPPA APEX II diffractometers, respectively. The SMART[21] program was used for collecting frames of data, indexing the reflections, and determination of lattice parameters, the SAINT[21] program for integration of the intensity of reflections and scaling, and the SADABS[22] program for absorption correction. The structures were solved by direct methods (SHELXS-97) and standard Fourier techniques and refined on F^2 using full-matrix least-squares procedures (SHELXL-97) using the SHELX-97 package[23] incorporated into WinGX.[24] Structural illustrations were drawn using ORTEP-3 for Windows.[25] All non-hydrogen atoms for both samples were refined anisotropically, except for the oxygen atoms in the solvent molecules. Hydrogen inclusion was done as per an earlier procedure.[18] To account for the unresolved solvent molecules in **2a**, the SQUEEZE (PLATON) program[26] was used. Crystallographic details of the structure analyses are summarized in Table 1.

Oxidation of Alcohols (Typical Procedure). In a stirred solution of benzyl alcohol (0.5 mL, 5 mmol) in acetonitrile (5 mL)

(21) *SMART & SAINT Software Reference Manuals, Version 5.0*; Bruker AXS Inc.: Madison, WI, 1998.

(22) Sheldrick, G. M. *SADABS, Bruker Nonius Area Detector Scaling and Absorption Correction*, version 2.05; University of Göttingen, Göttingen, Germany, 1999.

(23) Sheldrick, G. M. *Acta Crystallogr*. **2008**, *A64*, 112–122.

(24) Farrugia, L. J. *WinGX: An Integrated System of Windows Programs for the Solution, Refinement and Analysis for Single Crystal X-ray Diffraction Data*, version 1.80.01; Department of Chemistry, University of Glasgow, Glasgow, Scotland, 2003. (Farrugia, L. J. *J. Appl. Crystallogr*. **1999**, *32*, 837−838).

(25) Farrugia, L. J. ORTEP-3 for Windows, version 2.01. *J. Appl. Crystallogr*. **1997**, *30*, 565.

(26) Spek, A. L. *Acta Crystallogr*. **1990**, *A46*, C34.

Scheme 1

$$Co(NO_3)_2\cdot 6H_2O + NaO_2CC_6H_4\text{-}X + L \xrightarrow[H_2O_2\ (30\%,\ v/v)]{MeOH} Co_4O_4(O_2CC_6H_4\text{-}X)_4(L)_4$$

1a-e and 2a-e

Where,

L = py (**1**) and 4-Mepy (**2**)

X = H (**a**); Me (**b**); OMe (**c**); Cl (**d**); NO_2 (**e**)

was suspended 10 mg (~0.2 mol %) of the complex; 2 mL of aqueous *tert*-butyl hydroperoxide (TBHP, 70%) was then added, and the resultant mixture was stirred at 82 °C. For other alcohols equivalent amounts were used. The reaction progress was monitored by TLC in all cases and also by GC in selected cases. At the completion of the reaction, the excess TBHP was destroyed by adding sodium metabisulfite. After removal of solvent, the crude product was purified by flash chromatography.

Results and Discussion

Syntheses and Characterization of Complexes. The Co(III) clusters **1a**−**e** and **2a**−**e** have been prepared by chemically oxidizing 1:2:1 mixtures of $Co(NO_3)_2\cdot 6H_2O$, NaO_2CAr, and N-donor ligands (pyridine or 4-methylpyridine) in methanol (Scheme 1). The preparative method developed by us is quite general and reproducible. Complex **1a** was earlier reported to have formed as $Co_4O_4(py)_4(O_2CPh)_4\cdot 4CH_3CN\cdot 4H_2O$ during H_2O_2 oxidation of a cobalt(II) dimer.[27]

All complexes precipitate out from the reaction mixtures as dark green products in moderate to very good yield. The vacuum-dried samples in all cases correspond to the general formula $Co_4O_4(O_2CC_6H_4\text{-}X)_4(L)_4$, as indicated by analytical as well as ESI-MS results (Supporting Information). The purity and analogous nature of the species are also supported by their electronic and ^1H NMR spectra (see below). In addition, the mid-IR spectral data given in the Experimental Section are quite informative regarding the nature of ligands present in the complexes. As described earlier,[18,28] we note here that from among the three characteristic peaks observed in the region 550−700 cm^{-1} the moderate intensity band near 635 cm^{-1} is attributable to the Co(III)−oxo stretching vibration of the cubane core of the complexes. All the compounds are soluble in common organic solvents in varying degrees, with the solubility decreasing in solvents of higher polarity. The complexes are essentially insoluble in water; however, some of them (e.g., **1a**) have appreciable solubility in diethyl ether. This is in contrast with their acetate analogues, $Co_4O_4(O_2CMe)_4L_4$ (where L = py, 4-Mepy, 4-Etpy, 4-CNpy), which are moderately soluble in water.[18]

The electronic spectra for **1a**−**e** (top) and **2a**−**e** (bottom) are shown in Figure 1. The observed maxima along with respective molar absorption coefficients, ε (M^{-1} cm^{-1}), are given in Table 2. Three absorption maxima are seen in the spectra, which are quite analogous as expected. For the complexes **1a**−**e**, the absorption maxima associated with the d−d transition involving either $^1A_1 \rightarrow {}^1T_1$ or $^1A_1 \rightarrow {}^1T_2$ for the approximately octahedral d^6-Co(III) centers (low spin) in solution are observed in the 623−646 nm range. For complexes **2a**−**e** the λ_{max} values for the d−d transition are found to be between 605 and 638 nm. The other two bands are attributable to origins other than ligand-field transitions. The band at ~360 nm is associated with a charge transfer transition involving the μ_3-O−Co(III) moiety present in the complexes. The λ_{max} values range from 353 to 362 nm and from 343 and 362 nm for **1a**−**e** and **2a**−**e**, respectively. The highest energy band is of ligand origin, and it occurs between 236 and 273 nm for **1a**−**e** and between 235 and 273 nm for **2a**−**e**. The observed shift to higher frequency is dependent on the nature of the substituent present at the para position of the aryl group of the carboxylato ligand. A red shift in the order of $-NO_2$ (273 nm) > −OMe (257 nm) > −Me (244 nm) ≈ −Cl (244 nm) > −H (236 nm) is observed for complexes **1a**−**e** (Figure 1, top). Similar variations in the highest energy band are also observed for **2a**−**e** (Figure 1, bottom). The UV−visible spectral data for complexes **1** and **2** are analogous to results described earlier for other complexes of the same type.[18]

The molecular structures of two representative compounds (**1a** and **2a**) have been determined by single-crystal X-ray diffraction. Crystallographic details are available in Table 1 in the Experimental Section, while ORTEP representations are provided as Supporting Information. Selected bond distances and angles for complexes **1a** and **2a**, which are also summarized in the Supporting Information, show that the bond parameters are comparable to those for the acetate analogues described earlier.[18] The minor structural differences may be ascribed to the presence of different ligands and solvent molecules in the crystals. In both cases the Co(III) centers are found to occur in distorted-octahedral coordination environments. In the "Co_4O_4" cube, there are two long Co···Co distances and four short Co···Co distances to indicate a negative S_4 distortion[29] due to the compression along the S_4 symmetry of the inner Co_4 tetrahedron. The shorter Co···Co separations correspond to edges bridged by both O_2^- and $PhCO_2^-$.

The diamagnetic nature of the complexes, as expected for cobalt(III) ions with a low-spin d^6 electron configuration, are reflected in the ^1H NMR spectra recorded for $CDCl_3$ solutions of **1a**−**e** and **2a**−**e**. The proton resonances are summarized in Table 3. The para-substituted −Me and −OMe groups of the carboxylato ligands for **1c**,**d** resonate at 2.32 and 3.79 ppm, respectively.

(27) Karmakar, A.; Sarma, R. J.; Baruah, J. B. *Polyhedron* **2007**, *26*, 1347–1355.

(28) Eppley, H. J.; Tsai, H.-L.; de Vries, N.; Folting, K.; Christou, G.; Hendrickson, D. N. *J. Am. Chem. Soc.* **1995**, *117*, 301–317.

(29) Isele, K.; Gigon, F.; Williams, A. F.; Bernardinelli, G.; Franz, P.; Decurtins, S. *Dalton Trans.* **2007**, 332–341.

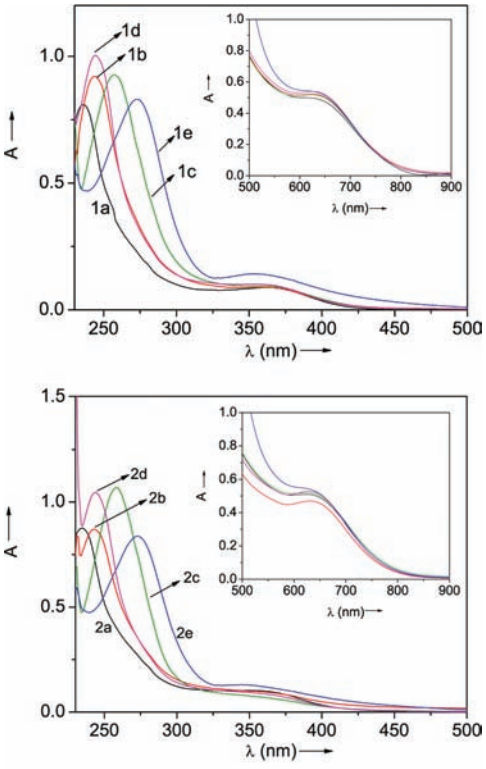

Figure 1. Electronic spectra of (top) $Co_4(\mu_3\text{-}O)_4(\mu\text{-}O_2CC_6H_4\text{-}X)_4(py)_4$ (**1a**−**e**) and (bottom) $Co_4(\mu_3\text{-}O)_4(\mu\text{-}O_2CC_6H_4\text{-}X)_4(4\text{-}Mepy)_4$ (**2a**−**e**) in CH_2Cl_2 solutions (10^{-5} M). Insets: spectra for 10^{-3} M solutions.

The spectra in all cases may be interpreted easily. The appearance of a single set of resonances for all four benzoates as well as pyridines in each complex is consistent with the virtual T_d symmetry of the molecules in solution. It also indicates the stability and integrity of the complexes in solution. Furthermore, the simplicity of the spectra observed for the complexes suggests that complexes of other nuclearities are not present as impurities in the bulk samples obtained by us. This is in contrast to earlier observations, where species of different nuclearities were observed.[30]

Electrochemical Properties. Electrochemical behavior of **1a**−**e** and **2a**−**e** in dichloromethane under dry anaerobic conditions has been studied by cyclic voltammetry (CV) and differential pulse voltammetry (DPV). The cyclic voltammograms for both series of complexes are very similar, each showing distinct anodic and cathodic peaks. The complexes in the series **1** and **2** undergo a one-electron oxidation in the potential ranges +0.74−1.0 V and +0.71−0.96 V vs SCE, respectively (Table 4). Since the ligands involved are redox-inactive in the applied potential window, the electrochemical processes must arise from the metal-based redox reactions. Examples of CV and DPV curves are provided as Supporting Information. The cyclic voltammogram of **1a** exhibits a redox couple with $E_{1/2} = 0.78$ V vs SCE. While the peak-to-peak separation ($\Delta E_p = E_{pa} - E_{pc}$) for the observed voltammogram is 0.17 V, the ratio of cathodic to anodic current (i_{pc}/i_{pa}) is ~1.0. Considering that the i_{pc}/i_{pa} value is indicative of reversibility of the redox couple,

Table 2. Electronic Spectral Data on Complexes $Co_4(\mu_3\text{-}O)_4(\mu\text{-}O_2CC_6H_4\text{-}X)_4(py)_4$ (**1a**−**e**) and $Co_4(\mu_3\text{-}O)_4(\mu\text{-}O_2CC_6H_4\text{-}X)_4(4\text{-}Mepy)_4$ (**2a**−**e**) in CH_2Cl_2

complex	λ_{max} (CH_2Cl_2), nm (ε, M^{-1} cm^{-1})
1a	634 (490), 361 (10 700), 236 (80 000)
1b	623 (522), 362 (8599), 244 (92 120)
1c	623 (518), 360 (10 046), 257 (92 620)
1d	625 (539), 353 (12 346), 244 (100 420)
1e	646 (sh), 355 (13 857), 273 (83 070)
2a	624 (509), 353 (sh), 235 (87 610)
2b	631 (470), 362 (sh), 243 (87 070)
2c	605 (sh), 362 (sh), 258 (106 930)
2d	630 (528), 360 (sh), 244 (104 610)
2e	638 (sh), 343 (13 016), 273 (83 770)

the observed ΔE_p values not only for this particular complex but also for all the other cubane complexes in both series of compounds (Table 4) are rather high for reversible redox behavior. In the scan rate range 5−20 mV s^{-1} explored for **1a** (see the Supporting Information), the ΔE_p value increases from 0.11 V at 5 mV s^{-1} to 0.17 V at 20 mV s^{-1}, indicating the quasi-reversibility of the process. In MeCN, however, the ΔE_p value observed for complex **2a** is much lower at 82 mV ($E_{1/2} = 0.77$ V). Similar lower ΔE_p values of 66 and 73 mV were also found for the complex $[Co_4(\mu_3\text{-}O)_4(\mu\text{-}O_2CMe)_4(py)_4]$ using MeCN as the solvent, utilizing Pt and glassy carbon, respectively, as working electrodes.[18] In view of the above results it may be said that the oxidation of cubane clusters of the type $Co^{III}{}_4(\mu_3\text{-}O)_4(\mu\text{-}O_2CR)_4L_4$ is a slow process in dichloromethane medium but is fast enough to make the redox process nearly reversible in acetonitrile medium. The necessary structural reorganization of the inner Co_4O_4 cubane following the transfer of an electron is believed to be the reason behind the slow heterogeneous electron transfer process.

The DPV trace of **1a** gives a peak potential (0.80 V) which is close to the value obtained from CV measurement. On teh basis of the stoichiometry of electron transfer determined from the peak current measurements using ferrocene in equimolar concentration as an internal standard, the electron-transfer process involves a one-electron oxidation of the cubane core from $[Co^{III}{}_4(\mu_3\text{-}O)_4]^{4+}$ to $[Co^{III}{}_3Co^{IV}(\mu_3\text{-}O)_4]^{5+}$. Electrochemical studies of the structurally related complex $[Co_4(\mu_3\text{-}O)_4(\mu\text{-}O_2CMe)_4(bpy)_2]^{2+}$ by Christou et al.[31] and also by us[18] have shown similar redox behavior involving the tetrameric cubane core. The near-reversibility of the redox process suggests that both oxidized and native species are stable under the conditions applied.

In our attempts to correlate the observed electrochemical redox potentials with the particular chemical species under study, it was found instructive to examine the effect of the carboxylato ligands on the redox behavior shown by the complexes. The variation of the remote para substituent on the bridging carboxylate ligand has a profound effect on the observed redox potentials for both series of complexes. Plots of Hammett σ_p parameters for the substituents versus the observed $E_{1/2}$ values for the redox couples for **1a**−**e** (top) and **2a**−**e** (bottom) are shown in Figure 2. Potentials increase linearly as a function of σ_p, giving a

(30) Beattie, J. K.; Klepetko, J. A.; Masters, A. F.; Turner, P. *Polyhedron* **2003**, *22*, 947–965.

(31) Dimitrou, K.; Brown, A. D.; Concolino, T. E.; Rheingold, A. L.; Christou, G. *Chem. Commun.* **2001**, 1284–1285.

Table 3. ^{1}H NMR Spectral Data for Complexes **1a**−**e** and **2a**−**e** in $CDCl_3$

complex	δ(py/4-Mepy), ppm	δ($ArCO_2^-$), ppm
1a	8.72 (d, *J* = 4 Hz, 8H), 7.35 (t, *J* = 4 Hz, 4H), 7.02 (t, *J* = 8 Hz, 8H)	8.01 (d, *J* = 4 Hz, 8H), 7.50 (t, *J* = 8 Hz, 4H), 7.24 (t, *J* = 8 Hz, 8H)
1b	8.74 (d, *J* = 4.8 Hz, 8H), 7.47 (t, *J* = 7.2 Hz, 4H), 7.04 (t, *J* = 8 Hz, 8H)	7.93 (d, *J* = 8.0 Hz, 8H), 6.98 (t, *J* = 6.8 Hz, 8H), 2.32 (s, 12H)
1c	8.75 (d, *J* = 5.2 Hz, 8H), 7.48 (t, *J* = 7.6 Hz, 4H), 6.99 (t, *J* = 6.4 Hz, 8H)	7.99 (d, *J* = 8.8 Hz, 8H), 6.73 (d, *J* = 8.8 Hz, 8H), 3.79 (s, 12H)
1d	8.70 (d, *J* = 4.9 Hz, 8H), 7.52 (t, *J* = 7.7 Hz, 4H), 7.01 (t, *J* = 6.4 Hz, 8H)	7.97 (d, *J* = 8.5 Hz, 8H), 7.21 (d, *J* = 8.5 Hz, 8H)
1e	8.69 (d, *J* = 5.2 Hz, 8H), 7.58 (t, *J* = 7.2 Hz, 4H), 7.07 (t, *J* = 6.4 Hz, 8H)	8.21 (d, *J* = 8.4 Hz, 8H), 8.12 (d, *J* = 8.4 Hz, 8H)
2a	8.55 (d, *J* = 5.2 Hz, 8H), 6.83 (d, *J* = 5.6 Hz, 8H), 2.33 (s, 12H)	8.03 (d, *J* = 7.2 Hz, 8H), 7.34 (t, *J* = 7.2 Hz, 4H), 7.23 (t, *J* = 7.2 Hz, 8H)
2b	8.55 (d, *J* = 4 Hz, 8H), 6.79 (d, *J* = 4 Hz, 8H), 2.30[a] (s, 24H)	7.92 (d, *J* = 8 Hz, 8H), 7.01 (d, *J* = 8 Hz, 8H)
2c	8.53 (d, *J* = 4 Hz, 8H), 6.81 (d, *J* = 4 Hz, 8H), 2.30 (s, 12H)	7.97 (d, *J* = 8 Hz, 8H), 6.72 (d, *J* = 8 Hz, 8H), 3.77 (s, 12H)
2d	8.50 (d, *J* = 4 Hz, 8H), 6.83 (d, *J* = 4 Hz, 8H), 2.33 (s, 12H)	7.95 (d, *J* = 8 Hz, 8H), 7.18 (d, *J* = 8 Hz, 8H)
2e	8.49 (d, *J* = 4 Hz, 8H), 6.89 (d, *J* = 4 Hz, 8H), 2.37 (s, 12H)	8.19 (d, *J* = 8 Hz, 8H), 8.11 (d, *J* = 8 Hz, 8H)

[a] The methyl protons from 4-Mepy and *p*-methylbenzoate are not resolved and appear as a merged singlet.

Table 4. CV[a] and DPV[b] Data for **1a**−**e** and **2a**−**e** in CH_2Cl_2/0.1 M TBAP vs SCE

	CV data		
complex	$E_{1/2}$ (V)	ΔE_p (mV)	DPV data (V)
1a	0.78	170	0.80
1b	0.77	118	0.78
1c	0.74	158	0.75
1d	0.87	172	0.88
1e	1.00	198	1.02
2a	0.77	114	0.79
2b	0.71	150	0.72
2c	0.71	128	0.73
2d	0.83	172	0.84
2e	0.96	244	0.96

[a] Scan rate 20 mV s^{-1}. [b] Scan rate 5 mV s^{-1}.

measure of electronic influence of the substituents on $E_{1/2}$. The electrochemical potentials in both series of complexes increase in the following order: OMe < Me < H < Cl < NO_2. While the −MeO and −Me groups are electron releasing in nature in aromatic systems, −Cl and $-NO_2$ groups are electron withdrawing. As the ligand becomes more electron releasing, the increased electron density at the metal center makes the Co(III) center in the complex easier to oxidize and more difficult to reduce. Earlier electrochemical studies on $[M_2(O_2CR)_4]^{0/+}$ complexes revealed similar linear dependence of the electrochemical potentials on the para substituents of aryl carboxylato ligands.[32] Manchanda has also reported that the rate of electron transfer is retarded by more electron withdrawing substituents on the bridging carboxylates in oxo-centered trinuclear iron complexes.[33] Plots of $E_{1/2}$ versus pK_a values of the carboxylic acids also correlate linearly for both series of complexes.

Catalytic Study. The oxidation of alcohols to the corresponding carbonyl compounds remains one of the most basic chemical transformations from both fundamental research and synthetic points of view.[34] However, many of the traditional processes for alcohol oxidation use forcing conditions and toxic stoichiometric oxidants.[35] In view of this, development of green, efficient, and selective catalyst systems using benign oxidants continues to remain an important goal. The research efforts making use of both homogeneous[36] and heterogeneous[37] catalysts for this reaction have been reviewed recently. Several systems for the aerobic oxidation of alcohols using cobalt-based homogeneous catalysts have appeared recently.[36−41] In a previous paper we have shown that a heterogeneous catalyst prepared by immobilizing the complex $Co^{III}_4(\mu_3\text{-}O)_4(\mu\text{-}O_2CMe)_4(py)_4$ on chemically modified mesoporous silica efficiently and selectively catalyzes the oxidation of alcohols with nonaqueous TBHP as the oxidant.[19] Although there are indications that the metal complex present in the heterogenized system is closely related to the starting cubanelike complex, the catalytic behavior of the cubane complexes per se in the TBHP oxidation of alcohols has not been examined in detail so far. Herein we describe our preliminary results on the use of complexes **1a**−**e** and **2a**−**e** as

(32) (a) Chisholm, M. H.; Glasgow, K. C.; Klein, L. J.; Macintosh, A. M.; Peters, D. G. *Inorg. Chem.* **2000**, *39*, 4354–4357. (b) Das, B. K.; Chakravarty, A. R. *Inorg. Chem.* **1991**, *30*, 4978–4986.
(33) Manchanda, R. *Inorg. Chim. Acta* **1996**, *245*, 91–95.
(34) (a) Arends, I. W. C. E.; Sheldon, R. A. In *Modern Oxidation Methods*; Bäckvall, J.-E., Ed.; Wiley-VCH: Weinheim, Germany, 2004; pp 83−118. (b) Larock, R. C. Comprehensive Organic Transformations, 2nd ed.; Wiley-VCH: New York, 1999.
(35) Smith, M. B.; March, J. *March's Advanced Organic Chemistry: Reactions, Mechanisms and Structure*, 6th ed.; Wiley-Interscience: Hoboken, NJ, 2007; pp 1715−1728.
(36) (a) Schultz, M. J.; Sigman, M. S. *Tetrahedron* **2006**, *62*, 8227–8241. (b) Zhan, B.-Z.; Thompson, A. *Tetrahedron* **2004**, *60*, 2917–2935.
(37) (a) Alaerts, L.; Wahlen, J.; Jacobs, P. A.; De Vos, D. E. *Chem. Commun.* **2008**, 1727–1737. (b) Mallat, T.; Baiker, A. *Chem. Rev.* **2004**, *104*, 3037–3058.
(38) Iwahama, T.; Yoshino, Y.; Keitoku, T.; Sakaguchi, S.; Ishii, Y. *J. Org. Chem.* **2000**, *65*, 6502–6507.
(39) (a) Sharma, V. B.; Jain, S. L.; Sain, B. *J. Mol. Catal. A: Chem.* **2004**, *212*, 55–59. (b) Das, S.; Punniyamurthy, T. *Tetrahedron Lett.* **2003**, *44*, 6033–6035.
(40) Sharma, V. B.; Jain, S. L.; Sain, B. J. *Mol. Catal. A: Chem.* **2005**, *227*, 47–49.
(41) Partenheimer, W. *Adv. Synth. Catal.* **2006**, *348*, 559–568.

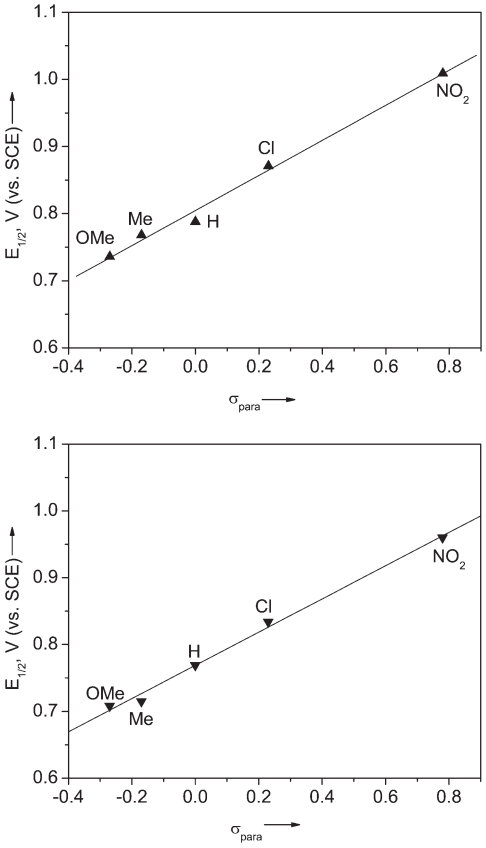

Figure 2. Correlation of Hammett constants σ_p for the para substituents on the aryl carboxylates with midpoint potentials ($E_{1/2}$) in complexes **1a**−**e** (top) and **2a**−**e** (bottom).

homogeneous catalysts in the oxidation of a few benzylic alcohols with aqueous TBHP, as illustrated by Scheme 2 for benzyl alcohol.

Typically we dissolved 5 mmol of a given substrate in 5 mL of acetonitrile with a catalytic amount (0.2 mol %) of the chosen Co(III)−cubane complex in the series $Co_4O_4(O_2C_6H_4\text{-}X)_4(L)_4$. The solution was heated to 82 °C and treated with 2 mL of the TBHP (70%, aqueous) oxidant. The reaction products were isolated using the procedure mentioned in the Experimental Section. The reaction at room temperature was slow and yielded only 33% of benzaldehyde from benzyl alcohol after 24 h with **1a** as the catalyst. However, the conversion increased remarkably at the reflux temperature of MeCN (82 °C) to yield 92% benzaldehyde as the isolated product. Thus, we chose 82 °C as the standard reaction temperature for the rest of our study. When the amount of catalyst was varied from 2 mg to 10 mg, the yield of benzaldehyde increased from 29 to 92% (Figure 3). A further increase in catalyst amount (up to 15 mg) did not show significant enhancement in yield of the product. Moreover, variation of the amount of TBHP also had a significant effect on the productivity of benzaldehyde (Supporting Information). The product yield rose with TBHP amount from 0.5 to 2.0 mL, but the increase in yield on changing the TBHP amount from 2.0 to 2.5 mL was marginal. Hence, we used 2 mL of TBHP for 10 mg of **1a** and equivalent amounts (~2 mol %) of the other complexes.

The progress of the oxidation of benzyl alcohol using complex **1a** as the catalyst, as monitored by gas

Scheme 2

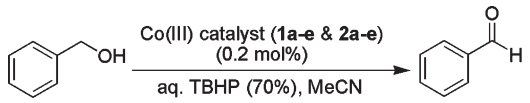

chromatography, is shown in Figure 4. It suggests that the conversion of benzyl alcohol is nearly quantitative, with benzaldehyde as the major product along with benzoic acid as the minor product. Using **1a** as the catalyst, benzaldehyde forms in 93% yield after 5 h with 7% of benzoic acid as the only other product. The conversion of benzyl alcohol proceeds almost linearly with time for the first 3 h, and thereafter the production of benzaldehyde levels off. The selectivity toward benzaldehyde remains almost constant at ~90% throughout the course of the reaction. The TOF value calculated at the end of 5 h is found to be 110 h^{-1}.

As shown by the results of our studies summarized in Table 5, all the complexes under study are highly active as catalysts. The benzaldehyde yields in all cases are the isolated yields calculated after separating the products by flash chromatography. It is important to note that under optimized conditions the reactions are essentially complete in all cases. Product yields may be assumed to be lower than quantitative, due to the fact that some amount of benzoic acid also forms during the reactions. It is also notable that the present results are uniformly better compared to the observed yield (60%) of benzaldehyde in a previously reported[19] homogeneous reaction catalyzed by the complex $Co_4(\mu_3\text{-}O)_4(\mu\text{-}O_2CMe)_4(py)_4$. The benzaldehyde yields found using complexes **1a**−**e** and **2a**−**e** as homogeneous catalysts are in fact comparable to the best yield found using the heterogeneous catalyst based on the above cubane complex. The catalytic performance of these Co(III)−oxo cubane complexes in the oxidation of alcohols is also comparable to that of other recently reported systems that use Co-based catalysts. Ishii et al.[38] have shown that Co(III) complexes in combination with *N*-hydroxyphthalimide (NHPI) catalyze the oxidation of a variety of alcohols. However, use of additives and undesirable solvents to achieve high yield and selectivity in such processes makes our results more attractive from an atom economy point of view. Co(II)−Schiff base complexes[39] also have been recently shown to catalyze the aerobic oxidation of alcohols. The Co(II)-based catalysts, however, need addition of bromide ion as the promoter for catalytic efficiency.[40,41]

With the above optimized conditions, we have extended the process to a few other benzylic alcohols, which also undergo facile oxidation in the presence of **1a** as the catalyst. The results are summarized in Table 6. The data show that complex **1a** efficiently and selectively catalyzes the oxidation of para-substituted benzylic alcohols (Table 6, entries 1 and 2) with TBHP as the oxidant. Furthermore, it also acts as a very good catalyst for the oxidation of secondary alcohols (Table 6, entries 3−5). In all cases the corresponding aldehydes were the main products with the corresponding carboxylic acid as the minor product. Our results on the TBHP oxidation of alcohols thus clearly indicate the usefulness of the cobalt(III)−oxo cubane clusters as promising catalysts or catalyst precursors.

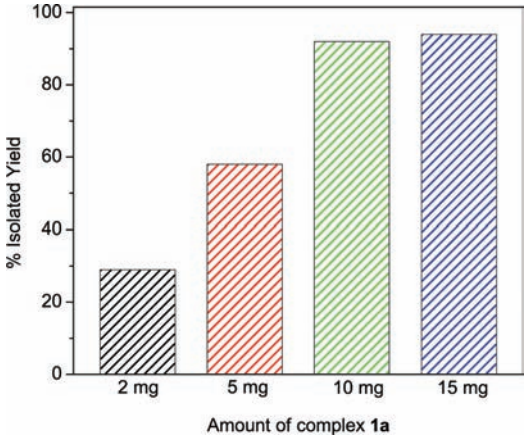

Figure 3. Effect of catalyst concentration on benzyl alcohol oxidation with complex **1a** as the catalyst in MeCN at 82 °C.

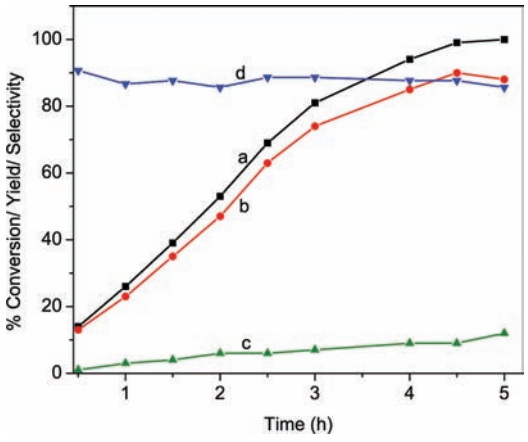

Figure 4. TBHP oxidation of benzyl alcohol with **1a** as the catalyst: (a) percent conversion of benzyl alcohol; (b) percent yield of benzaldehyde; (c) percent yield of benzoic acid; (d) percent selectivity for benzaldehyde. Reaction conditions: catalyst, 0.2 mol %; TBHP, 2 mL; MeCN, 5 mL; temperature, 82 °C.

Mechanistic aspects of the reaction described above are not clear at this stage. In view of the fact that in the absence of the cobalt complex (**1a**) only 2% conversion of benzyl alcohol is observed, a catalytic role of the cobalt(III) complexes is clearly indicated in alcohol oxidation. Under similar conditions the same reaction was carried out using a solution of a Co(II) salt containing pyridine. At the end of 5 h we noted a benzaldehyde yield of ~25%, which is quite low compared to the situation where the Co(III) cubanes were used. In order to understand the possible steps involved in the TBHP oxidation of benzylic alcohols catalyzed by Co(III)−oxo cubane clusters, we carried out a few control experiments. The stability of the complex $Co_4(\mu_3\text{-}O)_4(\mu\text{-}O_2CC_6H_5)_4(py)_4$ (**1a**) was tested variously by refluxing 0.3 g samples separately for 3 h in 20 mL volumes of (i) acetonitrile, (ii) benzyl alcohol, (iii) 70% aqueous TBHP, (iv) acetonitrile + benzyl alcohol, and (v) acetonitrile + TBHP. In all cases we could isolate pure solid samples of **1a** from the above mixtures. Also, the UV−visible spectra of the filtrates correlated well with the expected spectrum of the starting complex. In addition, the UV−visible spectrum of the complex in acetonitrile remains qualitatively the same after addition of a small volume of TBHP into the solution (λ_{max} changes from 634 to 627 nm for this ill-defined peak). No spectral changes were observed, even after heating the above solution containing TBHP. These observations appear to suggest that the cobalt(III)−cubane complex is unreactive toward the reactants and solvents used in the organic transformation reported by us in this paper.

Table 5. Catalytic Effect of Complexes **1a**−**e** and **2a**−**e** in the TBHP Oxidation of Benzyl Alcohol[a]

entry	complex	amt of complex, mg (~0.2 mol %)	amt of TBHP, mL	yield, %[b]
1	**1a**	10	2.0	92
2[c]	**1a**	10	2.0	33
3	**1b**	11	2.0	83
4	**1c**	12	2.0	88
5	**1d**	12	2.0	94
6	**1e**	13	2.0	96
7	**2a**	11	2.0	90
8	**2b**	12	2.0	85
9	**2c**	13	2.0	87
10	**2d**	13	2.0	93
11	**2e**	13	2.0	95

[a] Reaction conditions: benzyl alcohol, 0.55 g (5 mmol); acetonitrile, 5 mL; reaction time, 5 h; reaction temperature, 82 °C. [b] Isolated benzaldehyde yields. [c] Room-temperature reaction.

In order to examine whether autoxidation could be involved in the oxidation reaction under study, we carried out a control reaction under an atmosphere of N_2 gas to find a maximum conversion close to what was found in the presence of air. In the absence of TBHP no reaction was found to take place in air. Moreover, it may be reiterated that both substrate conversion and product yield depend on the amount of TBHP used in the reaction. Thus, it appears likely that no autoxidation is responsible for the reported conversion of benzyl alcohol mediated by the Co(III)−oxo cubanes.

The true identity of the dissolved complex remaining in the reaction mixture at the end of the reaction has not been established as yet. However, although the color of the solution is somewhat more brownish, the electronic spectrum of the solution in the visible region remains practically unchanged. We were able to isolate the metal complex from the chromatographic column with MeCN, and the resultant greenish brown solution showed an absorption at 642 nm, which is close to 634 nm, where an MeCN solution of complex **1a** absorbs. It is believed that the complex may not be identical with the cubane complex used, but it is likely to be a closely related species having the cubane-like "Co_4O_4" core.

Metal-catalyzed oxidations with hydrogen peroxide or alkyl hydroperoxides are generally divided into two categories, depending on the kind of active oxidant involved in the reaction. While reactions involving an oxometal species entail a two-electron oxidation, the peroxometal pathway does not involve any change in oxidation state of the metal during the catalytic cycle.[42] No stoichiometric oxidation of substrates is expected in the latter pathway. As shown in the Electrochemical Properties section above, the cubane complexes utilized by us as catalysts undergo only a one-electron oxidation. Furthermore, in the absence of the TBHP oxidant no

(42) Sheldon, R. A.; Arends, I.; Hanefeld, W. *Green Chemistry and Catalysis*; Wiley-VCH: Weinheim, Germany, 2007; pp 170−185.

Table 6. Oxidation of Benzylic Alcohols using Complex **1a** as the Catalyst with TBHP as Oxidant[a]

Entry	Substrate	Product	Time (h)	Yield[a] (%)
1	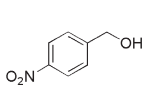	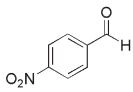	5	93
2	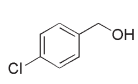	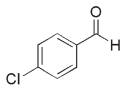	5	89
3			4	90[b]
4	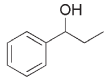	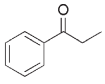	5	84[b]
5	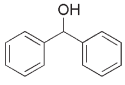	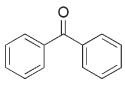	7	83

[a] Reaction conditions: substrate, 5 mmol; acetonitrile, 5 mL; catalyst amount, 0.2 mol %; TBHP amount, 2 mL; reaction temperature, 82 °C.

stoichiometric oxidation of the alcohols takes place. Thus, we believe that a peroxometal pathway is likely to be involved in the alcohol oxidation reactions mediated by the cobalt(III)−oxo cubane clusters **1** and **2**. Provided that this pathway is followed by the reactions studied by us, it is imperative that a Co(III)−*tert*-butylperoxo complex would be involved as an intermediate species in the reaction. Such species may be stabilized and isolated under suitable conditions.[43] In view of the role of alkylperoxo complexes in the decomposition of ROOH,[44] this proposed catalytic pathway appears to be quite plausible.

Conclusion

Tetrameric cobalt(III)−oxo clusters having aryl carboxylates and pyridines as ligands exhibit physicochemical properties dependent on electronic effects of the substituents present at the 4-position of the phenyl ring. The electrochemical studies show a linear relationship between the redox potentials and the Hammett σ_p parameters for the para substituents on the carboxylato ligands. Catalytic test reactions have shown that these complexes are quite effective in the TBHP oxidation of benzylic alcohols under homogeneous conditions, which is likely to proceed via a peroxometal pathway.

Acknowledgment. Financial assistance from the DST, Government of India, is gratefully acknowledged. We thank Prof. A. R. Chakravarty of the Indian Institute of Science for allowing R.C. to make use of electrochemical instrumentation in his laboratory. P.S. thanks the Council of Scientific and Industrial Research (New Delhi) for the award of a research fellowship.

Supporting Information Available: CIF files giving complete structural results for **1a**·6MeOH·0.5H_2O and **2a**·3.5MeOH·5H_2O, ESI-MS of **1b**−**e** (Figures S1−S5) and **2a**−**e** (Figures S6−S10), ^{1}H NMR spectra of **1b**−**e** (Figures S11−S15) and **2a**−**e** (Figures S16−S20), ORTEP diagrams for **1a**·6MeOH·0.5H_2O and **2a**·3.5MeOH·5H_2O (Figures S21 and S22), selected interatomic distances and angles for **1a**·6MeOH·0.5H_2O and **2a**·3.5MeOH·5H_2O (Table S1), cyclic and differential pulse voltammograms for complex **1a** (Figures S23 and S24), correlation graphs of Hammett constants σ_p with pK_a in complexes **1a**−**e** (Figure S25) and **2a**−**e** (Figure S26), and a bar diagram showing the effect of the amount of oxidant on benzyl alcohol oxidation (Figure S27). This material is available free of charge via the Internet at http://pubs.acs.org.

(43) Chavez, F. A.; Mascharak, P. K. *Acc. Chem. Res.* **2000**, *33*, 539−545 and references therein.

(44) Saussine, L.; Brazi, E.; Robine, A.; Mimoun, H.; Fischer, J.; Weiss, R. *J. Am. Chem. Soc.* **1985**, *107*, 3534–3540.